Raymo, M.E., Jansen, E., Blum, P., and Herbert, T.D. (Eds.), 1999
Proceedings of the Ocean Drilling Program, Scientific Results, Vol. 162

6. PLIOCENE–PLEISTOCENE AND REDEPOSITED DINOFLAGELLATE CYSTS FROM THE WESTERN SVALBARD MARGIN (SITE 986): BIOSTRATIGRAPHY, PALEOENVIRONMENTS, AND SEDIMENT PROVENANCE[1]

Morten Smelror[2]

ABSTRACT

The distribution of dinoflagellate cysts in the upper Pliocene and Pleistocene succession at Site 986 is influenced by depositional processes attributed to the formation of a fan complex near the mouth of the Storfjorden Trough and by climatological and oceanographic processes controlling glacial buildup in the Barents Sea. More than 290 taxa have been identified from Hole 986C, compared to 208 different taxa from Hole 986D. Most of these taxa are reworked from older Neogene, Paleogene, and Mesozoic deposits. A provenance on the central to eastern Barents Shelf and/or eastern Svalbard, following a westerly drainage route toward the major depositional fans along the western shelf margin, is suggested. The biostratigraphy of selected Pliocene–Pleistocene dinoflagellate species, together with data from magnetostratigraphy and foraminifers, provides information on the ages of the sediments. Biostratigraphic events recognized at Site 986 are correlated with datums previously reported from the Vøring Plateau in the Norwegian Sea and the Yermak Plateau north of Svalbard.

Fluctuations in the relative abundance of various taxa and variations in the gonyaulacoid/peridinioid dinoflagellate cyst ratio are used to identify changes in the paleoenvironments through the upper Pliocene–Pleistocene succession. Glacial depositional conditions were established from 2.3 to 2.4 Ma, but the marine microfloras suggest a relatively strong influence of the North Atlantic Current during periods of the late Pliocene–early Pleistocene and that comparatively warm surface-water masses were transported by the West Spitsbergen Current. These periods of warm water inflow must have alternated with periods of continuous sea-ice cover in the Arctic Ocean. Glacial depositional conditions prevailed through the Pleistocene. The abundance and diversity of dinoflagellate cysts are generally low in these deposits, but levels with increased richness, combined with the occurrence of typical outer neritic to oceanic species, suggest periods with inflow of warmer Atlantic water masses. Such events are noted at ~1.5, 1.2, and 0.5 Ma.

INTRODUCTION

In recent years the Cenozoic sedimentary succession on the western Barents Shelf and Svalbard margin has attracted considerable interest. The Cenozoic history of this area has been influenced by extensive shelf erosion, associated with redeposition on the slope and in the basins of the evolving Norwegian-Greenland Sea to the west (Fig. 1). The magnitude, timing, and causes of uplift and consequent erosion became a matter of considerable interest and debate when the Barents Shelf was opened for petroleum exploration after 1980. This is because late-phase Cenozoic erosion is thought to have significantly affected the petroleum accumulated in the traps. The history of research (and results from recent studies on the impact of glaciations on the Barents Shelf and Svalbard margin) has been presented by Solheim et al. (1996).

The establishment of a stratigraphy for the Cenozoic sequences on the outer shelf edge has been difficult. The extensive reworking of microfossils, especially in the younger depositional sequences, has on several occasions led to serious misinterpretations. Although the early work was concerned with an erosion phase that was assumed to predate the glacial period, Eidvin and Riis (1989) and Eidvin et al. (1993) suggested that most of the sedimentary wedge on the southwestern margin of the Barents Sea was of Pliocene–Pleistocene age and of glacial origin. Eidvin et al. (1993) based their work on investigations of exploration wells on the Senja Ridge (including 7117/09-01). They were later supported by Mørk and Duncan (1993) and Sættem et al. (1994) on information from shallow cores drilled in the Bear Island West area, and by Eidvin et al. (1998) from study of the deep exploration well 7316/05-01. The chronostratigraphy of the depositional units identified along the margin, however, is not yet fully resolved.

Site 986 is located between two glacial fans north of the main depositional wedges off the Storfjorden Trough and Bear Island Trough (Figs. 1, 2). The site has a good seismic control. By dating the major reflectors, the onset and main phases of glacial erosion and deposition can be detailed and the history of the Svalbard-Barents Ice Sheet established. The major objective of this dinoflagellate study has been to aid age determination of the seismic sequences. However, variations in the composition of the dinoflagellate assemblages have also been used to interpret environmental conditions during deposition of the main sedimentary sequences. Reworked palynomorphs provide additional information on the erosion history and indicate the provenance of the eroded sedimentary rocks.

SEISMIC SEQUENCES AND CHRONOSTRATIGRAPHY OF HOLE 986

The upper Cenozoic succession drilled at Site 986 penetrates all the main regional seismic reflectors (R1–R7) of the Svalbard-Barents Shelf margin (Faleide et al., 1996). These allow a subdivision of the sedimentary succession into eight seismic sequences, of which the upper seven are believed to be glacial in origin (Figs. 2, 3). A description of the seismic sequences is found in Jansen, Raymo, Blum, et al. (1996). The cored succession at Site 986 is divided into four main lithostratigraphic units (I–IV). The lower unit was further subdivided into two subunits (IVA and IVB) (Fig. 3). Only the lithostratigraphic boundaries between Units II and III and between Subunits IVA and IVB correlate with seismic boundaries (i.e., Reflectors R6 and R7, respectively) (Jansen, Raymo, Blum, et al., 1996).

The chronostratigraphy and evidence for age determination of the different seismic sequences are discussed by Channell et al. (Chap. 10, this volume). Although the dinoflagellate zonations defined for the Norwegian-Greenland Sea by Mudie (1989; Leg 104, Sites 642–

[1]Raymo, M.E., Jansen, E., Blum, P., and Herbert, T.D. (Eds.), 1999. *Proc. ODP, Sci. Results*, 162: College Station, TX (Ocean Drilling Program).

[2]The Norwegian University of Science and Technology (NTNU), Museum of Natural History and Archaeology, Erling Skakkes gt. 47, N-7004 Trondheim, Norway.
morten.smelror@vm.ntnu.no

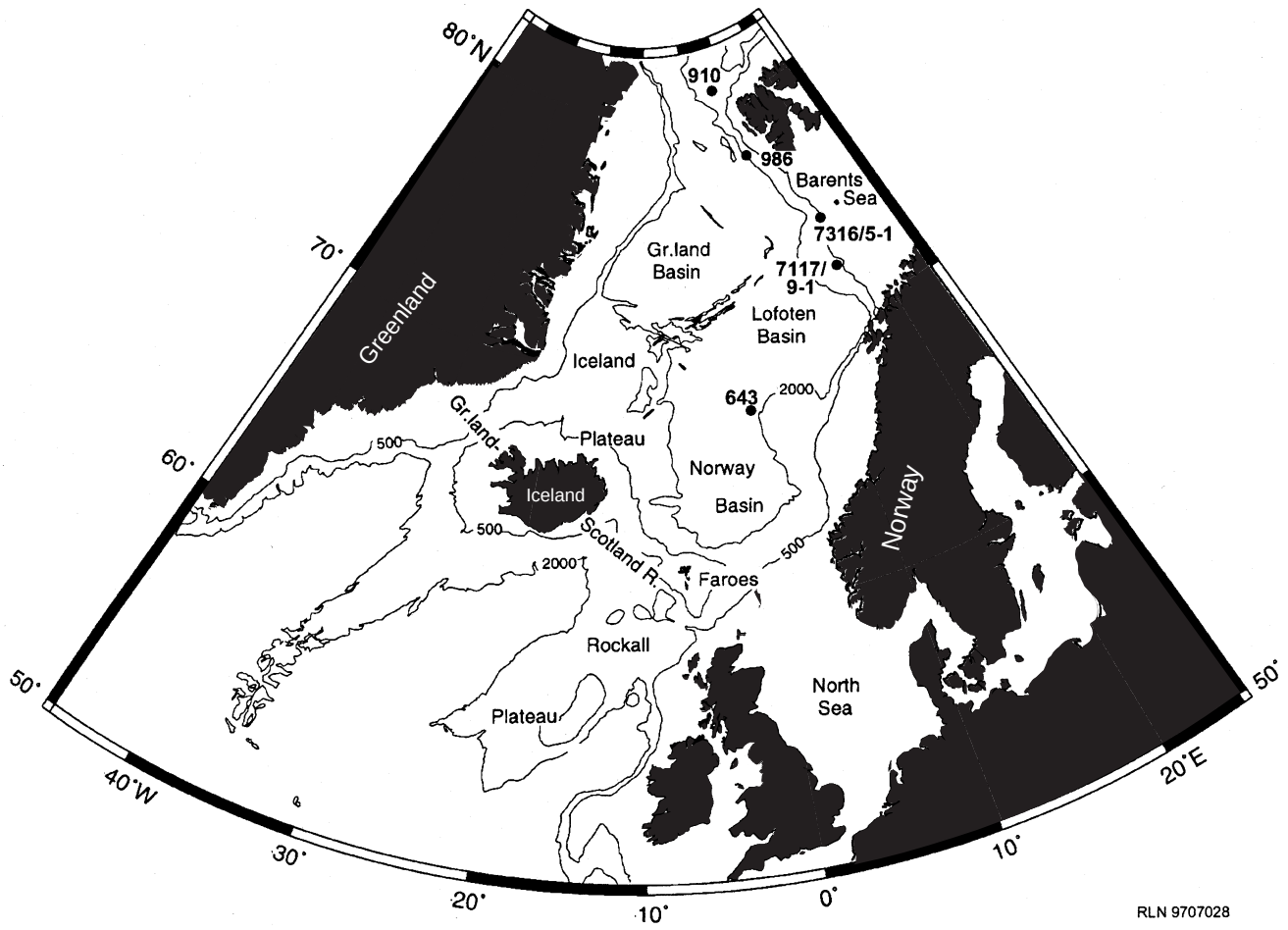

Figure 1. Map of the North Atlantic Ocean showing the location of Site 986 and other wells/boreholes discussed in the text (see also Fig. 6 for details).

644) and Poulsen et al. (1996; Leg 151, Sites 907–909, 913) may prove applicable for the upper Cenozoic of the Svalbard-Barents Shelf margin, the dinoflagellate biostratigraphy herein is discussed in relation to the identified seismic sequences. Biostratigraphic correlations with other Ocean Drilling Program (ODP) sites are based on selected dinoflagellate events that may or may not correspond to zonal markers used in the definition of the previously published zonations.

MATERIALS AND METHODS

Four holes were drilled at Site 986, with a maximum penetration of 964.6 meters below seafloor (mbsf). Samples used for palynological analyses are from Holes 986C (0–402.67 mbsf) and 986D (387.80–964.6 mbsf). One sample of ~5 cm^3 was taken from each core, and a total of 82 samples was selected for palynological analysis (Table 1). The samples were processed at the University of Oslo, following traditional methods including HCl, HF, ultrasonic treatment, and sieving at 20 µm. No oxidation or staining was applied. A set of three slides was made for each sample; all three slides were examined for dinoflagellate cysts.

In addition to identification of different dinoflagellate species, semiquantitative estimates based on counts of 150 to 200 specimens were made for each sample. With such a count and with generally <15 in situ species present, the true proportion will occur between 3% and 9% at either side of the estimated percentage at two standard deviations, depending on the actual number of specimens counted (Van der Plas and Toby, 1965; Harland, 1984). A more accurate comparison with the data sets published by Mudie (1989) for the Norwegian Sea (Vøring Plateau) and Matthiessen and Brenner (1996) for the Yermak Plateau would result if numbers of cyst/gram of sediment had been calculated. The Pliocene–Pleistocene off western Svalbard, however, represents sediments derived from a margin with high depositional rates and sedimentological processes different from those acting on the hemipelagic sedimentation at the Vøring Plateau and Yermak Plateau.

The generic allocation and authorship of dinoflagellate cyst taxa follow Lentin and Williams (1993), except where otherwise stated.

DINOFLAGELLATE CYST BIOSTRATIGRAPHY

Stratigraphic distribution charts for the dinoflagellate cysts recovered from Holes 986C and 986D are presented in Appendixes A and B (on back-pocket foldout, this volume). Dinoflagellate cysts are recovered from all 82 examined samples. Preservation is generally good, but abundance and species diversity vary significantly throughout the studied Pliocene–Pleistocene succession. More than 290 different taxa of dinoflagellate cysts have been identified from Hole 986C (38 samples), and 208 different taxa have been recovered from Hole 986D (44 samples). A number of species have been identified only to genus level, and several species are listed under open nomenclature in the range charts. As pointed out by Mudie (1989), many species found in the Neogene of the Norwegian-Greenland Sea

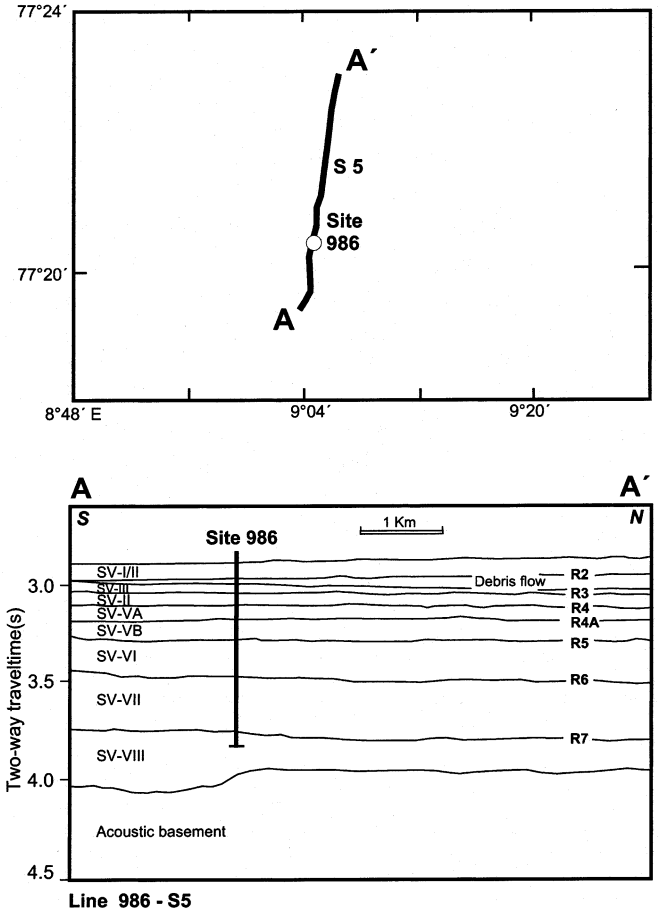

Figure 2. Position of Site 986 on seismic Line 986-S5 and the stratigraphic position of the drilled succession related to the seismic reflectors and seismic units recognized at the drill site (after Jansen, Raymo, Blum, et al., 1996).

are still not formally described. To some extent, this hampers the potential use of Neogene dinoflagellate cysts for biostratigraphy and regional correlations. One important observation from this site, however, is that most of the taxa recovered from Holes 986C and 986D are not in situ but reworked Mesozoic and Paleogene dinoflagellates. Although the diversity of in situ taxa seems to decline upward into the Pleistocene, the total diversity of recovered species shows a more erratic picture. Periods with extensive reworking on the Barents Shelf and Svalbard can apparently be related to periods with extensive erosion and reworking following the change to glacially dominated depositional regimes in the late Pliocene–Pleistocene.

Seismic Unit SV-VIII (Oceanic Basement to 871 mbsf; late Pliocene)

The lower boundary of this seismic unit corresponds to the basement estimated at 1170 mbsf; the top corresponds to seismic Reflector R7 (Fig. 2). This onlaps an elevated block of the oceanic basement east of the Knipovich Ridge (Myhre and Eldholm, 1988). Estimates of the spreading rate suggest that the ridge block is not older than 5–6 Ma (Sundvor and Eldholm, 1979; Hjelstuen et al., 1996). Farther south in the Lofoten Basin, the termination of Reflector R7 onto oceanic basement indicates that this seismic boundary is not older than 5.2 Ma (Fiedler, 1992).

Hole 986D was terminated at 964.6 mbsf, whereas the lowest palynological sample is from 955.74 mbsf. The age of this lowest sample is difficult to date. The marker species having their last appearance datums (LADs) at the top of Zone Mio6 of Poulsen et al. (1996) have not been found in Unit SV-VIII, indicating that this unit is not as old as the NN 11 Zone. The presence of *Sumatradinium pliocenicum* Head 1993 throughout this unit further supports an age not older than early Pliocene, but the total range of this species is presently not well documented (Head, 1993). *Filisphaera filifera,* which Mudie (1989) used as a marker for her *Filisphaera filifera*-PM2 Zone, has its lowest occurrence at 909.14 mbsf. The base of the PM2 Zone was calibrated to ~4.2 Ma based on magnetostratigraphic data. More recent observations, however, suggest that *F. filifera* also ranges into the upper (and mid?) Miocene (Poulsen et al., 1996).

Reticulatosphaera actinocoronata is common from the lowest investigated samples at 955.74 m up to 909.14 mbsf, where the species has its last in situ occurrence. Poulsen et al. (1996) used the last occurrence of this species to define the top of their Pli1 Zone of early Pliocene age (dated as equivalent to the NN 12–14 Zones). In contrast, Mudie and Harland (1996) placed the LAD of *R. actinocoronata* at the top of the Olduvai magnetostratigraphic Subchron, suggesting a significantly younger age for this dinoflagellate LAD. Further, according to Mudie and Harland (1996), *Invertocysta lacrymosa* also has its LAD at the top of the Olduvai Subchron. In Hole 986D, this species has its highest occurrence at 909.14 mbsf. An age as young as late Pliocene (~1.65 Ma) at this level is, however, not supported by foraminifer biostratigraphy (Eidvin and Nagy, Chap. 1, this volume), magnetostratigraphy, and seismic correlations (Channell et al., Chap. 10, this volume). It should be noted that Poulsen et al. (1996) used the LAD of *Invertocysta lacrymosa* to define the top of their Pli3 Zone of late Pliocene age (equivalent to NN 16–18 Zones). In a recent study on the impact of the onset of major Northern Hemisphere glaciations on the dinoflagellate cyst assemblages in the Mediterranean and the North Atlantic (Site 607), Versteegh (1997) found that the LAD of *Invertocysta lacrymosa* appears to be a valuable marker for oxygen isotope Stage 110. If this is valid for Hole 986, then a late Pliocene age of ~2.74 Ma is suggested at 909.14 mbsf.

The LAD of *Selenopemphix brevispinosa* at 928.34 mbsf may prove to be a more reliable marker within Unit SV-VIII. According to Head (pers. comm., 1991), this species has its LAD within the early late Pliocene (e.g., beds correlatable to the NN 16 Zone). This event supports an age of ~2.6–2.7 Ma for the lowermost part Hole 986D.

Seismic Unit SV-VII (871–561 mbsf; late Pliocene)

The lower boundary of this unit corresponds to seismic Reflector R7. This reflector marks the onset of the major glacial sedimentation along the Svalbard-Barents Shelf margin. Based on the foraminifer biostratigraphy in wells on the Senja Ridge (Eidvin et al., 1993) and dating by Ar isotopes from a shallow borehole in the Bjørnøya West area (Mørk and Duncan, 1993), an age of ~2.3 Ma has been assigned to this reflector (Faleide et al., 1996). Paleomagnetic data suggest that the top of the Olduvai Chron can be placed at 735 mbsf in this zone, whereas the base of the Olduvai is found at 756 mbsf (Channell et al., Chap. 10, this volume) and hence have ages of ~1.77 and 1.95 Ma, respectively. The upper boundary of this unit corresponds to seismic Reflector R6 (Figs. 2, 3).

There are very few age-diagnostic dinoflagellate events recognized in this unit. In their study of the Pliocene–Pleistocene sequences during Leg 151, Hole 911A, on the Yermak Plateau, Matthiessen and Brenner (1996) noted a distinct abundance peak of *Filisphaera filifera* in the upper Pliocene. In Hole 986D, a small acme of this species is recognized at 804.84 mbsf. *Selenopemphix dioneaecysta* is also present up to 849.94 mbsf; to our knowledge, this species is not reported from post-Pliocene strata.

Sumatradinium pliocenicum is common and consistently present up to 564.44 mbsf, where it has its last occurrence. This species was

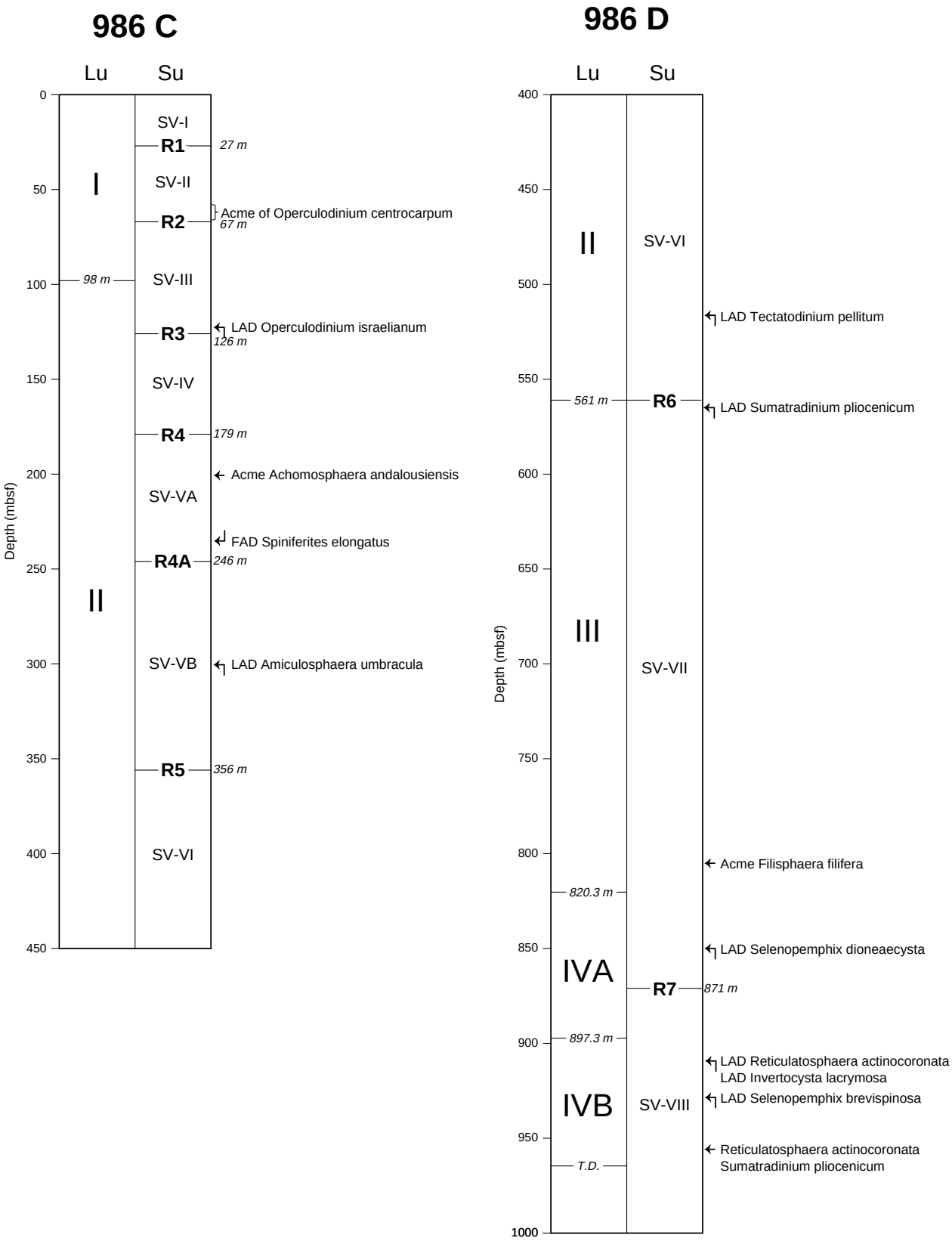

Figure 3. Lithostratigraphic units (LU), seismic units (SU), and main palynostratigraphic events in Holes 986C and 986D. R1 through R7 are seismic reflectors (see also Fig. 2).

originally described from the upper Pliocene of southwestern England and is not known to range above the Pliocene (Head, 1993). An age not younger than 1.65 Ma is thus suggested for the uppermost part of seismic Unit SV-VII.

Seismic Unit SV-VI (561–356 mbsf; early Pleistocene)

The lower boundary of this unit corresponds to seismic Reflector R6. The upper boundary is defined by Reflector R5 (Figs. 2, 3).

The age of this unit is difficult to interpret based on dinoflagellate cysts alone. The lower part of the unit is characterized by common to abundant *Brigantedinium* spp. and *Bitectatodinium tepikiense.* The LAD of *Tectatodinium pellitum* is noted at 516.44 mbsf. Poulsen et al. (1996) use the LAD of this species, together with the LADs of *Amiculosphaera umbracula, Filisphaera filifera, Impagidinium japonicum, I. multiplexum,* and *I. velorum,* to define the top of their Qty1 Zone (correlated to the NN 18 and 19 nannoplankton zones). *A. umbracula* is recognized in the lower part of Unit SV-VI but has its LAD in the overlying unit SV-VB (at 333.53 mbsf). Based on this, a general early Pleistocene age is suggested for this unit.

Seismic Unit SV-VB (356–246 mbsf; early Pleistocene)

The lower boundary of this unit corresponds to seismic Reflector R5. This reflector is recognized as an important seismic sequence boundary along the entire Svalbard-Barents Shelf margin (Faleide et al., 1996). Based on correlations with increased amounts of ice-rafted detritus and oxygen-isotope measurements elsewhere in the Norwegian-Greenland Sea, Faleide et al. (1996) assigned a likely age of 1.0 Ma to Reflector R5. The upper boundary of this unit is defined by seismic Reflector R4A (Figs. 2, 3).

The marine microfloras found in Unit SV-VB are broadly comparable to those of the underlying unit, although there appears to be a relative decline in the abundance of *Operculodinium centrocarpum* and *Spiniferites* spp. Age determinations based on dinoflagellate cysts are problematic, although the uppermost occurrence of *Amiculosphaera umbracula* at 333.53 mbsf may be taken as evidence of an early Pleistocene age at this level. Mudie and Harland (1996) questionably placed the LAD of this species at ~1.5 Ma. Poulsen et al. (1996) used, among others, the LAD of *A. umbracula* to define the top of their Qty1 zone, which they correlated with the top of the NN 19 Zone. An early Pleistocene age is therefore likely for Unit SV-VB.

Seismic Unit SV-VA (246–179 mbsf; early Pleistocene)

The lower boundary of this unit is defined by seismic Reflector R4A, whereas the upper boundary corresponds to Reflector R4 (Figs. 2, 3). Following the decline in numbers of dinoflagellate cysts at the top of the underlying unit, Unit SV-VA is characterized by relatively increased abundances of *Operculodinium centrocarpum, Spiniferites* spp., and *Bitectatodinium tepikiense.* The lowest occurrence of *Spiniferites elongatus* is observed at 235.44 mbsf. An acme of *Achomosphaera andalousiensis* is noted at 200.04 m.

An early Pleistocene age is assigned based on the unit's stratigraphic position above Reflector R5 and by the presence of *Operculodinium israelianum* throughout the unit. These factors suggest an early Pleistocene age, which is supported by measurements from the wireline logs indicating that the Cobb Mountain Event of 1.2 Ma can be recognized at around 200 mbsf.

Seismic Unit SV-IV (179–126 mbsf; early Pleistocene)

The lower boundary of this unit is defined by seismic Reflector R4; the upper boundary, by Reflector R3 (Figs. 2, 3). Channell et al. (Chap. 10, this volume) identified the top Jaramillo Event at 148 mbsf, giving an age of 0.99 Ma at this level. The Brunhes/Matuyama paleomagnetic boundary seems to be located at ~127 mbsf in this unit (Channell et al., Chap. 10, this volume). This event points to an age of 0.78 Ma at this stratigraphic level.

The dinoflagellate assemblages from this unit are, in overall character, comparable to those of the underlying unit. However, a marked decrease in the relative abundances of *Bitectatodinium tepikiense* and *Operculodinium centrocarpum* occur in the upper part of the unit. The presence of *Operculodinium israelianum* through this unit suggests a continuing assignment to the early Pleistocene.

Seismic Unit SV-III (126–67 mbsf; mid-Pleistocene)

The lower boundary of this unit is defined by seismic Reflector R3; the upper boundary corresponds to Reflector R2 (Figs. 2, 3). A mid-Pleistocene age of 0.46 Ma has previously been assigned to this unit based on the last occurrence of *Pseudomiliania lacunosa* at 125.83 mbsf (Jansen, Raymo, Blum, et al., 1996).

This unit differs from the underlying early Pleistocene units by containing lower abundances of the dinoflagellates *Bitectatodinium tepikiense* and *Operculodinium centrocarpum.* The relative proportion of *Brigantedinium* spp. appears comparable to those of the underlying Pleistocene units. *Spiniferites elongatus* is present throughout the unit. The LAD of *Operculodinium israelianum* at 122.18 mbsf indicate that the early/mid-Pleistocene boundary is close to this level. Harland (1992) and Mudie and Harland (1996) suggested that this species disappeared in the mid-Pleistocene in the North Atlantic region. This LAD gives an age of ~0.73 Ma at 122.18 mbsf, somewhat older than that suggested by the foraminifers.

Seismic Unit SV-II (67–27 mbsf; mid?-Pleistocene)

The lower boundary of Unit SV-II is defined by seismic Reflector R2; the upper boundary, by Reflector R1 (Figs. 2, 3).

An acme of *Operculodinium centrocarpum* and a minor abundance peak of *Spiniferites* spp. (including *S. elongatus*) are found in the lower part of the unit (66.04 mbsf). The abundance peak of *O. centrocarpum* is recorded between 66.04 and 58.04 mbsf. This may correlate with a comparable acme at 98.95 mbsf at Hole 911A on the Yermak Plateau. This event has been dated as 0.5 Ma (Matthiessen and Brenner, 1996).

Otherwise, Unit SV-II is characterized by low abundances of in situ dinoflagellate cysts. The LAD (a minor abundance peak) of *Filisphaera filifera* is also recognized at 66.04 mbsf. According to Mudie and Harland (1996), the LAD of this species is found near the base of the middle Pleistocene. An age as old as the base of the Brunhes magnetochron at 66.04 m, however, does not agree with the age determinations made for the underlying Unit SV-III.

Matthiessen and Brenner (1996) observed a distinct drop in the relative abundance of *Brigantedinium* spp. and an associated increase in the abundance of *Operculodinium centrocarpum* between 33.73 and 43.21 mbsf in Hole 911A on the Yermak Plateau. This turnover in assemblage was dated at ~0.5 Ma. A comparable change is observed at the transition between Units SV-III and SV-II in Hole 986C.

Seismic Unit SV-I (27–0 mbsf; late Pleistocene)

The lower boundary of Unit SV-I is defined by seismic Reflector R1 (Figs. 2, 3). The sediments above this reflector all belong to the Brunhes normal polarity epoch and must therefore be younger than 0.73 Ma (Channell et al., Chap. 10, this volume). Amino-acid analyses further indicate an age younger than 0.44 Ma (Faleide et al., 1996).

In situ dinoflagellate cysts are sparse in this unit but include characteristic taxa such as *Achomosphaera andalousiensis, Algidasphaeridium*? *minutum, Bitectatodinium tepikiense, Brigantedinium* spp., *Spiniferites elongatus, Operculodinium centrocarpum,* and *Nematosphaeropsis labyrinthea.* Most are taxa occurring in the western North Atlantic today. No exclusive Holocene taxa (like *Protope-*

ridinium oblongum) have been recovered, but the marked increase in the relative abundance of *O. centrocarpum* and *Spiniferites* spp. in the uppermost part of the unit (11.24–3.74 mbsf) may be attributed to the transition to the Flandrian.

REWORKING OF DINOFLAGELLATE CYSTS

The establishment of a Cenozoic biostratigraphy succession of the western Barents Shelf has been hampered by extensive reworking, especially in the younger sequences. Several controversies over the ages of the Cenozoic units have been caused by misinterpretation and miscorrelation of reworked microfaunas and -floras, which frequently comprise the dominant part of the assemblages. In the examined material from Site 986, the high number of species recorded (see range charts in Appendixes A and B) is a result of the dominant reworking of older Cenozoic and Mesozoic taxa. This is true for the whole cored succession and is especially typical for the units above Reflector R7. The relative abundances of reworked vs. in situ dinoflagellate cysts are shown in Figures 4 and 5.

The most commonly reworked dinoflagellate cysts in the upper Pliocene–lower Pleistocene of Hole 986D (Fig. 5) are of Cretaceous age. One interesting feature is the presence of Upper Cretaceous taxa at several levels (including *Diconodinium arcticum, Elytrocysta druggii, Heterosphaeridium difficile, Trithyrodinium verrucosum, Chatangiella granulifera, Chatangiella ditissima, Chlamydophorella*? *grossa,* and *Isabelidinium bakeri*). Today, Upper Cretaceous strata are missing on Svalbard, but reworked Upper Cretaceous dinoflagellate cysts are relatively common in the Paleogene sequences on Sørkapp Land on Spitsbergen. Reworked Paleogene forms are generally less frequent than Cretaceous taxa, but a peak abundance comprising 25% of the total dinoflagellate assemblage occurs in the sample at 679.94 mbsf. Jurassic dinoflagellates are rarer and in most samples comprise <2% of the total assemblages. A distinct acme of recycled Jurassic dinoflagellate cysts is, however, observed at 718.34 mbsf (including the species *Chlamydophorella ectotabulata, Chytroeisphaeridia cerastes, Paragonyaulacysta calloviense, Perisseiasphaeridium pannosum,* and *Sirmiodinium grossii*). The reworked Jurassic cysts are dominantly of post-Bathonian age and are probably derived from deposits of the Fuglen and Hekking Formations from the western Barents Shelf and/or the Janusfjellet Formation on eastern Svalbard.

The distribution pattern of reworked dinoflagellate cysts in the Pleistocene sediments of Hole 986C (Fig. 4) is broadly comparable to that of 986D. Recycled Cretaceous taxa are common, including both Lower and Upper Cretaceous species. Reworked Paleogene forms are most common above 200 mbsf but show a highly fluctuating distribution pattern. Jurassic specimens are generally less frequent than reworked Cretaceous and Paleogene forms but more common than in the older strata of Hole 986D. Distinct peak abundances of recycled Jurassic dinoflagellate cysts are recorded at 276.94 (28%), 267.34 (26%), 132.03 (16%), and 122.18 mbsf (19%). In contrast to Hole 986D, reworked Miocene dinoflagellates are found above 267.34 mbsf in Hole 986C, where they occur together with Paleogene and Mesozoic cysts. They are, however, rare and comprise only 1% to 2% of the total assemblage when present. A small increase in the relative abundance of recycled Miocene dinoflagellates (4%) is found in the uppermost studied sample at 3.74 mbsf.

In their study of the Miocene–Pleistocene of the De Soto Canyon, in the Gulf of Mexico, Wrenn and Kokinos (1986) recognized a correlation between reworked dinoflagellate cysts, carbonate fluctuations, and glacial cycles. The occurrence of reworked pre-Miocene dinoflagellate cysts was directly related to the abundance of clay/silt succession and inversely related to the carbonate content and coarse fraction percent. They concluded that if glacial–interglacial cycles determined the relative proportions of silt, clay, and carbonate in the Pliocene–Pleistocene of the Gulf of Mexico, then these cycles also controlled the influx of reworked dinoflagellate cysts. Because of the low sampling frequency, it is not possible to determine in detail the relationship between lithology and the relative proportions of reworked dinoflagellate cysts at Site 986. Obviously, however, there is a cyclicity in the abundance of both in situ and reworked dinoflagellate cysts in the upper Pliocene–Pleistocene (Figs. 4, 5). More data are needed before this can be evaluated further.

One interesting aspect is that the preservation of the reworked Mesozoic dinoflagellate cysts is generally very good. In contrast, dinoflagellate cysts from the Jurassic and Cretaceous formations on western and southern Spitsbergen are usually poorly preserved and have undergone moderate to high thermal maturation. Nonetheless, dinoflagellates from the Jurassic and Cretaceous of Kong Karls Land to the east in the Svalbard region, on Franz Josef Land, and on the shallow eastern parts of the Norwegian Barents Shelf are generally well preserved. This suggests a transport direction from the east toward the shelf margin and then following a northwest direction similar to the present West Spitsbergen Current (Fig. 6). Dinoflagellate cysts behave like fine silt particles in the water column and may be transported considerable distances in the ocean. A provenance area on the central to eastern Barents Shelf or eastern Svalbard, following a westerly drainage route toward the major depositional fans along the western shelf margin, is thus likely.

Willard (1996) suggested that reworked palynomorph assemblages from the Pliocene–Pleistocene at Sites 910 and 911 on the Yermak Plateau had their source on the Eurasian shelf, where they were either entrained within sea ice and transported via the Transpolar Drift or were conveyed in surface currents following a similar path. This assumption was based on the relationship of the reworked Upper Cretaceous pollen and spore assemblages to contemporaneous floras of the boundary between the Normapolles and *Aquilapollenites* Provinces in the Laptev Sea area. Upper Cretaceous terrestrial palynofloras comparable to those found reworked at Sites 910 and 911 are, however, also found in the marine Upper Cretaceous formations of the Norwegian Barents Shelf (i.e., Maud and Tromsø Basins). Reworked *Aquilapollenites* are also observed in the upper Pliocene–Pleistocene deposits at Site 986. The present observations suggest that the upper Cretaceous palynofloras and most of the other reworked Mesozoic palynomorphs at Site 986 came from the Barents Shelf via the main drainage areas into the Bjørnøya and Storfjorden Troughs (Nøttvedt et al., 1988) and were then transported with the West Spitsbergen Current into the depositional site west off Spitsbergen (Fig. 6).

DINOFLAGELLATE CYSTS AND PALEOENVIRONMENTAL INTERPRETATIONS

In recent years, dinoflagellate cysts have been used to interpret Neogene coastal, shelf, and deep-sea depositional environments of the Atlantic Ocean and adjacent seas (Harland, 1988; Mudie, 1989; de Vernal et al., 1992; McCarthy and Mudie, 1996; Matthiessen and Brenner, 1996; Versteegh, 1997; Zonneveld and Bossenkool, 1996) and to estimate shifts in paleotemperatures and ocean circulation patterns (Edwards et al. 1991; Mudie, 1992). Although the ecological preferences of most dinoflagellate cysts are not known in detail, the identified distribution pattern of many extant species found in Atlantic Ocean surface sediments (Mudie, 1992; Matthiessen, 1995; Dale, 1996) can be used to interpret the paleoenvironments of the upper Pliocene–Pleistocene succession at Site 986. There is an intimate relationship between dinoflagellate cyst assemblages and environmental conditions; further, regional ecostratigraphies reflect climatic changes with accuracy. It is also established that interpretations of Quaternary dinoflagellate cyst assemblages, based on the ecology of modern cysts, give results that are in good agreement with interpretations derived independently from oxygen isotope data, foraminifers, and coccolith microfloras (Mudie and Harland, 1996). As Mat-

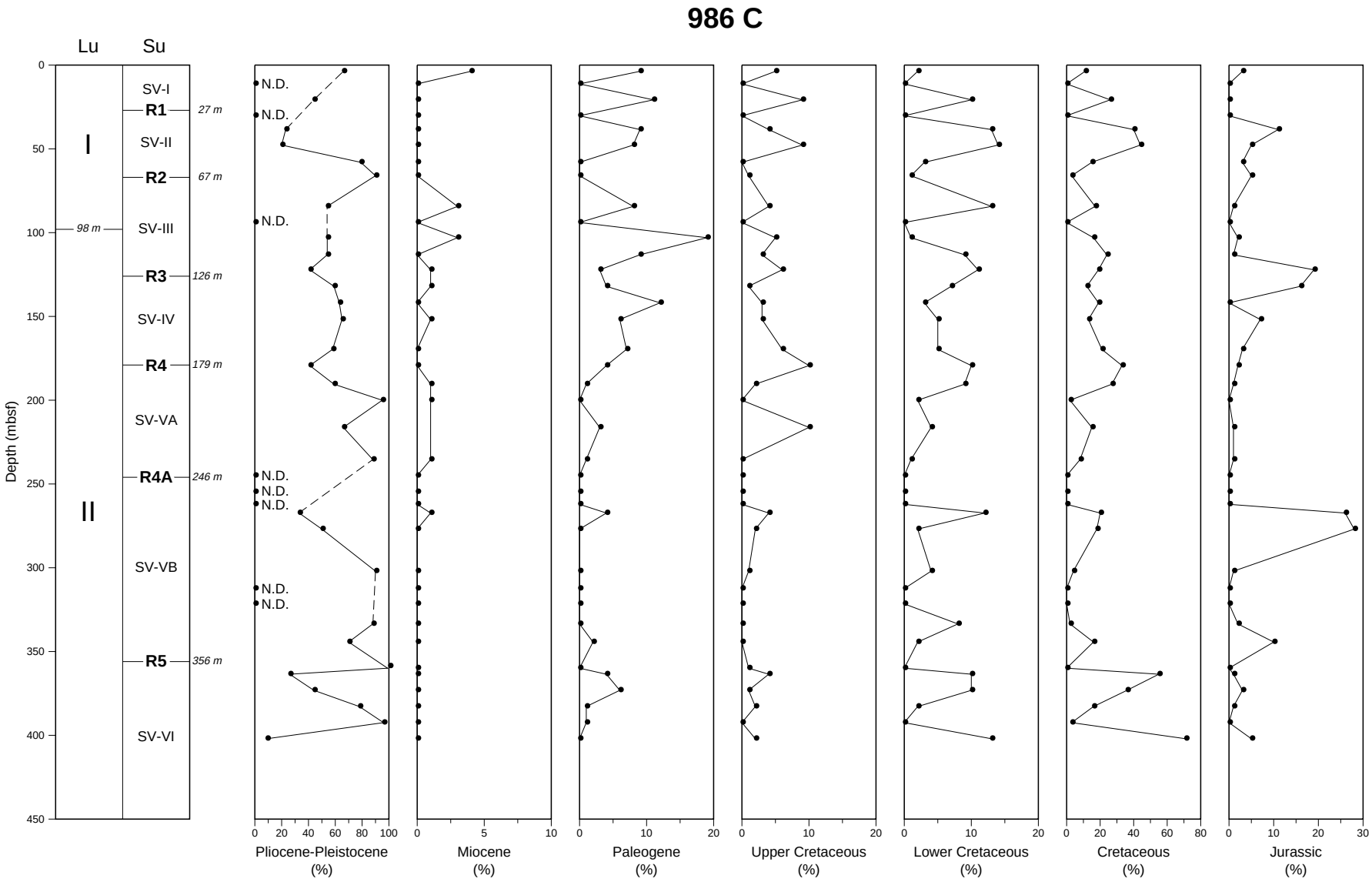

Figure 4. Relative abundances of upper Pliocene–Pleistocene and reworked Mesozoic dinoflagellate cysts in Hole 986C. N.D. = sample levels with low abundances of dinoflagellate cysts where no relative abundance data are calculated. LU = lithostratigraphic units, SU = seismic units. R1 through R5 are seismic reflectors.

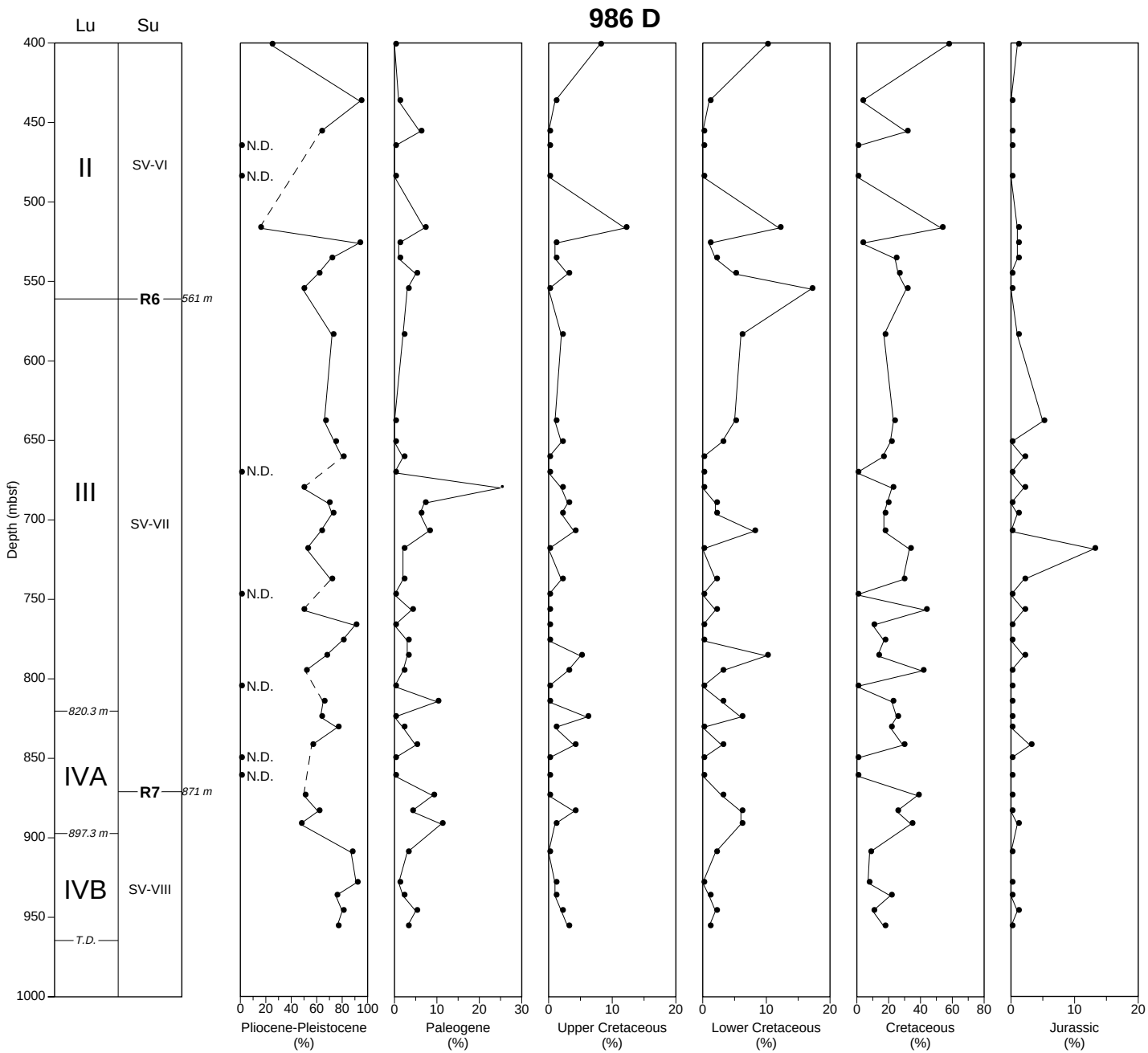

Figure 5. Relative abundances of upper Pliocene–Pleistocene and reworked Mesozoic dinoflagellate cysts in Hole 986D. R6 and R7 are seismic reflectors. Abbreviations as in Figure 4.

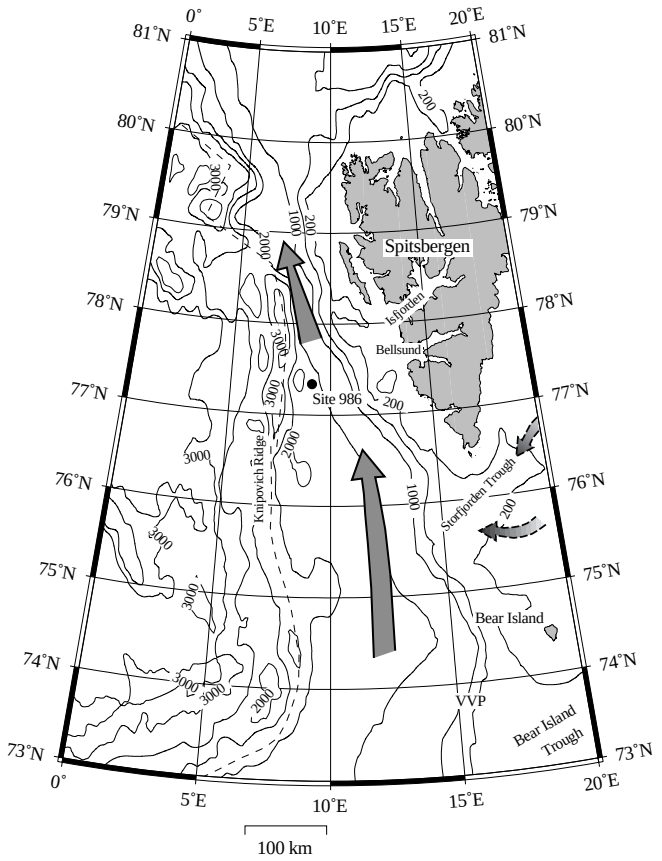

Figure 6. Position of Hole 986D in relation to the West Spitsbergen Current (black arrows to the left) and to the main transport direction of reworked dinoflagellate cysts from the western Barents Shelf through the Storfjorden Trough (gray arrows to the right). VVP = Vestbakken Volcanic Province.

thiessen and Brenner (1996) pointed out, however, it must be kept in mind that dinoflagellate cysts may be transported with surface and bottom currents over considerable distances, and that species preferring warmer water masses can be advected from the Norwegian Sea with the West Spitsbergen Current into the Arctic Ocean. Therefore, the dinoflagellate cyst record at Site 986 reflects not only local surface-water mass conditions but also regional changes in the West Spitsbergen Current and the North Atlantic Current. Thus, as in the approach used by Matthiessen and Brenner (1996), only changes in the abundance of taxa that are common to abundant are used to interpret changes in paleoenvironments through the upper Pliocene and Pleistocene succession.

In addition to determining fluctuations in the abundance of selected taxa, the gonyaulacoid to peridinioid value (G:P ratio) is used to detect changes in paleoenvironmental conditions in the upper Pliocene of Hole 986D. This ratio provides a rough index of surface-water temperature and sea-ice conditions (Edwards et al., 1991; Mudie, 1992; Mudie and Harland, 1996). Edwards et al. (1991) correlated five groups of G:P ratios with modern environments as follows: values <0.2 mark perennial pack-ice and arctic estuaries, ratios of 0.2–0.6 mark the seasonal ice zone, ratios of 0.8–2 characterize subarctic and transitional waters, and ratios greater than 4 indicate subtropical to tropical waters. The G:P ratios for Hole 986D are shown in Figure 7. At some levels with low counts of dinoflagellate cysts, the ratio has not been calculated. A major limitation of the G:P method is that the ratio often reflects other ecological factors. Low values may also indicate upwelling or deltaic conditions as well as the influx of large amounts of land-derived nutrients. According to Edwards et al. (1991), the method yields a very broad summer sea-surface tempera-

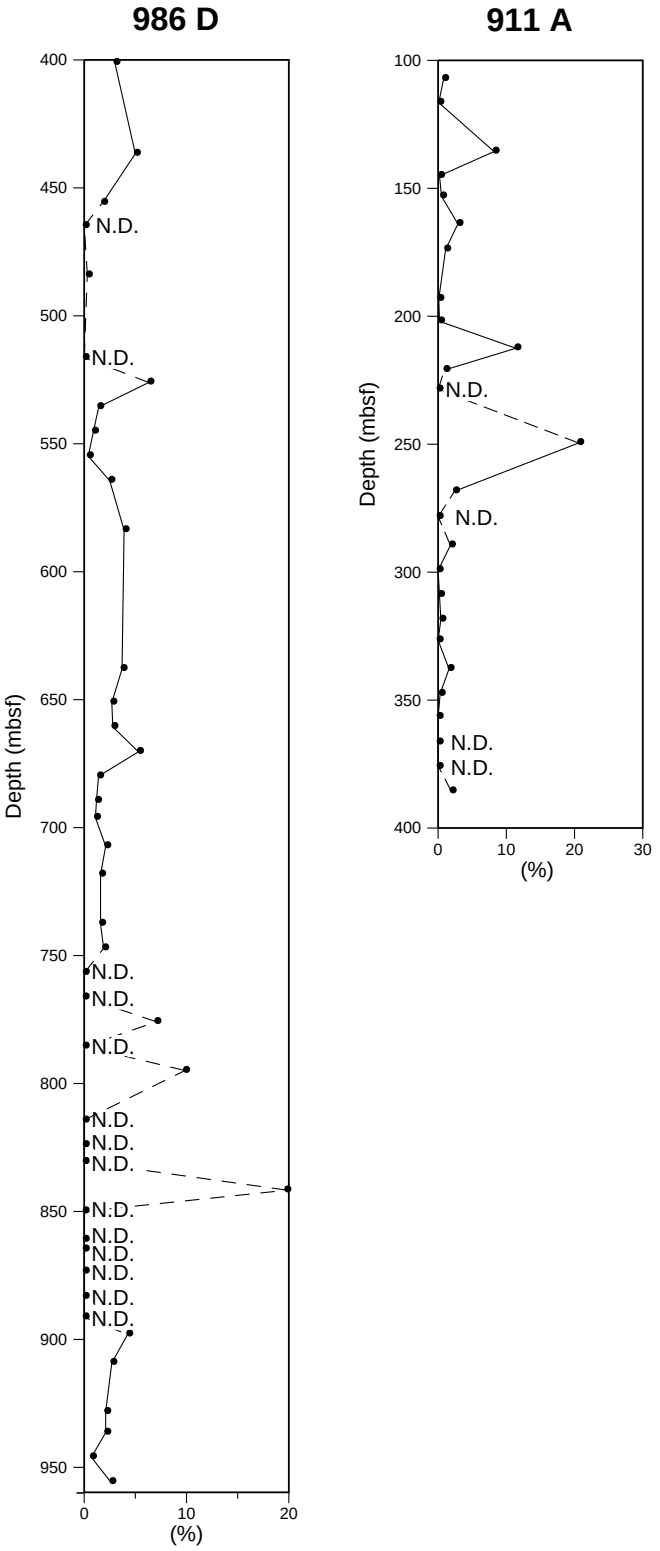

Figure 7. G:P ratios for the upper Pliocene–lowermost Pleistocene at Holes 986D and 911A. N.D. = sample levels with low abundances of in situ dinoflagellate cysts where no G:P ratios have been calculated.

ture of 14°–26°C only when protoperidinioids are rare or absent. Consequently, the method may be imprecise for larger parts of the upper Pliocene–Pleistocene succession at Site 986.

Late Pliocene (and earliest Pleistocene) Warm Events

Recent data from ODP Legs 151 in the Norwegian-Greenland Sea (Thiede and Myhre, 1996) and 152 off southeast Greenland (Larsen et al., 1994) have provided evidence that the middle Miocene was fairly mild, that cooling most likely started shortly after 10 Ma within the early late Miocene, and that full glacial conditions in southeast Greenland were not established until the middle part of the late Miocene. According to Thiede and Myhre (1996), the influence of sea ice and of the influx of icebergs, first from Greenland and later from northwestern Europe, increased during the Pliocene until it reached an important threshold ~3–4 Ma off southern Greenland and 2.6 Ma in the Fram Strait and off northwestern Europe.

The upper Pliocene sediment recovered below Reflector R7 at Site 986 (Unit SV-VIII) comprises silty clay, nearly barren of dropstones. High proportions of in situ dinoflagellates compared to reworked forms suggest a relatively low influence of redepositional processes compared to the overlying units. The relatively high diversity of in situ taxa and the high content of amorphous organic matter in the palynological preparations further support a hemipelagic depositional regime for these oldest sediments (Forsberg et al., Chap. 17, this volume). G:P ratios of dinoflagellate cysts are between 2 and 3, suggesting temperate to relatively warm sea-surface conditions. The sample at 946.04 mbsf, however, records a distinct cooling event, whereas one sample at 898.04 mbsf recorded a G:P ratio typical of subtropical to tropical waters. The most prominent gonyaulacoid taxa in Unit SV-VIII are *Operculodinium centrocarpum, O. israelianum, Spiniferites* spp., and *Reticulatosphaera actinocoronata*. A distinct acme of *Impaginidium patulum* is observed at 928.34 mbsf. *O. centrocarpum* is a ubiquitous species, tolerating a wide range of temperature and salinity conditions. This species is dominant in recent sediments from the Norwegian Sea (Matthiessen, 1995). In contrast, *O. israelianum* is a typical warm (temperate to tropical) species. The occurrence of this species supports the G:P ratio evidence of periods with warm water during the late Pliocene. The acme of *I. patulum* can be linked to the influx of oceanic water masses and suggests a strong influence of the North Atlantic Current during deposition of the sediments at 928.34 mbsf.

Unit SV-VIII also contains moderate counts of the protoperidinioids *Brigantedinium* spp. and *Selenopemphix brevispinosa*. Low-diversity dinoflagellate cyst assemblages with high quantities of *Brigantedinium* spp. are often a characteristic of polar to subpolar environments. However, assemblages dominated by *Brigantedinium* spp. are also common in temperate regions, especially in coastal upwelling areas (Wall et al., 1977). These assemblages, having a high diversity (especially of protoperidinioid cysts [Mudie, 1992; Mathiessen and Brenner, 1996]), differ from polar to subpolar ones. Thus, the presence of fairly common protoperidinioids in Unit SV-III does not contradict the overall picture of the influence of relatively warm water masses during deposition of the upper Pliocene clays.

Reflector R7 is interpreted to mark the onset of a major glacial wedge along the Svalbard-Barents Shelf margin. There are, however, no distinct changes in dinoflagellate assemblages and no marked lithologic changes across this seismic boundary. As in the underlying unit, *O. centrocarpum* and *Spiniferites* spp. are the most common taxa. *O. israelianum* is present throughout Unit SV-II, mostly in low numbers but with distinct abundance peaks at 830.64 mbsf and between 637.99 and 564.44 mbsf. Most notable is the absence of *Brigantedinium* spp. in the upper unit SV-III and in lower unit SV-II (up to 795.04 m).

The acmes of *O. israelianum* call for particular comment since these cysts suggest a distinct inflow of warm water into what is interpreted as a glacially dominated depositional area. These influxes of *O. israelianum* coincide with contemporaneous high abundances of this species at Sites 898 and 900, Leg 149, off Spain, in the late Pliocene to early Pleistocene (McCarthy and Mudie, 1996). The species is, however, only recorded in moderate to low numbers in the late Pliocene in southwestern and eastern England (Head, 1993, 1996, respectively) and in the late Pliocene to early Pleistocene of the Norwegian Sea (Mudie, 1989). Mathiessen and Brenner (1996) recorded low numbers of *O. israelianum* (as *O. crassum*) at two restricted intervals in the upper Pliocene and lower Pleistocene deposits at Hole 911A on the Yermak Plateau. These probably correlate with some of the warm-water influxes, which also are recorded at Site 986. Both the marked acme at 584.74 mbsf in the upper Pliocene at Site 986 and the minor abundance peak at 526.04 mbsf in the lower Pleistocene are accompanied by relatively high G:P ratios. The event at 526.04 mbsf corresponds to a similar and approximately contemporaneous event noted from 268.39 to 249.56 mbsf in Hole 911A on the Yermak Plateau (Fig. 7).

The record of warming episodes in the upper Pliocene–lowermost Pleistocene of Site 986 supports earlier observations from the Kap København Formation on Perry Land in North Greenland. Here Funder et al. (1985) recovered frequently well-preserved remains of terrestrial vegetation and invertebrate faunas indicative of a forested tundra environment intercalated within the glacial sequences. More recently, Willard (1996) recovered late Pliocene terrestrial microfloras at Sites 910 and 911, Leg 151, that are suggestive of open boreal vegetation with relatively temperate deciduous elements. These microfloras indicate warmer late Pliocene conditions in the source area adjacent to the Yermak Plateau. Similarly Spiegler (1996), Cronin and Whatley (1996), and Osterman (1996) recorded microfaunas typical of warm surface waters in upper Pliocene marine deposits at Site 910 on the Yermak Plateau. Based on these findings, Spiegler (1996) suggested that warm and subtropical surface-water masses invaded the generally cold Norwegian-Greenland Sea and Arctic Ocean in the late Pliocene during short-lived episodic events. This interpretation is supported by the results from Site 986, both from the dinoflagellate cyst record and from observation of the foraminifer fauna by Eidvin and Nagy (Chap. 1, this volume). The present data further suggest a relatively strong influence of the North Atlantic Current during periods of the late Pliocene to early Pleistocene and that warm surface-water masses were transported along the West Spitsbergen Current into the Fram Strait. These periods of warm-water inflow must have alternated with periods of continuous sea-ice cover in the Arctic Ocean (Matthiessen and Brenner, 1996).

Pleistocene Fluctuations

The Pleistocene sediments recovered at Site 986 are characterized by marked fluctuations in abundances of the dominant dinoflagellates *Brigantedinium* spp., *Bitectatodinium tepikiense*, *Spiniferites* spp., and *Operculodinium centrocarpum.* This compares well with the distribution pattern seen through the contemporaneous deposits at Hole 911A on the Yermak Plateau (Matthiessen and Brenner, 1996).

The sediments directly above seismic Reflector R6 (i.e., up to 526.04 mbsf) contain relatively high abundances of *Brigantedinium* spp., with the maximum at 545.24 mbsf. High abundances of these forms are often associated with polar to subpolar conditions. The occurrence of the distinct arctic species *Algidaspheridium*? *minutum* at 564.44 mbsf supports the influence of cold-water masses during deposition of these sediments. This species is only a minor constituent of the Pleistocene dinoflagellate assemblages at Site 986, but when present, it is generally associated with common *Brigantedinium* spp.

Between 535.64 and 526.04 mbsf, *Brigantedinium* is replaced by common to abundant *Bitectatodinium tepikiense.* This species has broad thermal tolerance but is absent or rare at present in the Arctic Ocean (Mudie, 1992; Matthiessen and Brenner, 1996). In the northwestern Atlantic, this species appears to prefer environments with cold winter and warm summer sea-surface temperatures (de Vernal et

al., 1992). According to Matthiessen and Brenner (1996), high percentage abundances of *B. tepikiense* are attributed to offshore mixing of polar-influenced oceanic waters with cold, brackish meltwaters from ice. They are associated with salinities around 30% and a relatively short seasonal sea-ice cover or even ice-free conditions.

Between 516.44 and 455.84 mbsf, there is a marked drop in the abundance of in situ dinoflagellates. The abundance of dinoflagellate cysts declines strongly with decreasing surface temperatures in polar regions; areas of permanent sea ice have <100 dinoflagellate cysts per gram, and most sediments under sea ice are barren (Mudie, 1992; Mudie and Harland, 1996). Quaternary glacial-stage sediments also have barren intervals, and the distinct drop in abundance between 516.44 and 455.84 mbsf can probably be related to a change to glacially dominated depositional conditions. Minor acmes in the distribution of *Brigantedinium* spp. and *Algidasphaeridium*? *minutum* at 484.18 mbsf appear to support this interpretation.

A new inflow of warmer surface-water masses is suggested by new high abundances of *Bitectatodinium tepikiense*, *Spiniferites* spp., and *Operculodinium centrocarpum*, and by the presence of *Operculodinium israelianum* at 436.64 mbsf. There also is an increase in the relative abundance of *Brigantedinium* spp. at this level, but the absence of *A.*? *minutum* supports the interpretation of a change to warmer conditions. The increased abundance of *Brigantedinium* spp. may here be attributed to increased nutrient levels, perhaps supplied from melting sea ice.

Fluctuations in the abundance of *Brigantedinium* spp., *Bitectatodinium tepikiense*, *Spiniferites* spp., and *O. centrocarpum* continue up to 151.84 mbsf (up to ~1.0 Ma). Low abundances and diversities of dinoflagellates suggest periods with cold conditions and low productivity during deposition of the sediments at 321.56–312.44 mbsf and 254.76–245.04 mbsf. High abundances of the three latter taxa indicate a change to warmer and more productive water masses during deposition of the sediments at 392.44–382.84, 353.94, 333.54, and 302.04 mbsf and from 235.44 to 151.84 mbsf.

Maximum abundance peaks of *Spiniferites* spp. and *O. centrocarpum* are seen at 200.04 mbsf. An age of 1.2 Ma has been assigned to the sediments at this level (Channell et al., Chap. 10, this volume). This event coincides with distinct acmes in the abundance of *Lingulodinium machaerophorum*, *Impagidinium aculetum*, *Spiniferites mirabilis*, and *Nematosphaeropsis labyrinthus*. Mudie and Harland (1996) described *L. machaerophorum* and *S. mirabilis* as typical cool-temperate to tropical species. According to Dale (1996), the consistent appearance of *L. machaerophorum* in interglacial sequences from Norway confirms the value of this species as an indicator of temperate or warmer waters. Mudie and Harland (1996) further describe *I. aculeatum* as a characteristic subtropical oceanic species, whereas *N. labyrinthus* is typical in temperate neritic to oceanic environments. Observations from Holocene sediments in the Norwegian-Greenland Sea and the Arctic Ocean, however, have shown that *N. labyrinthus* is also common in the cold-temperate gyres in the Greenland and Iceland seas, the subpolar gyre, and the eastern Arctic Ocean (Mudie, 1992; Matthiessen, 1995). The combined dinoflagellate evidence, however, suggests a period with inflow of temperate to warm North Atlantic water masses into the West Spitsbergen Current around 1.2 Ma.

Above 141.89 mbsf, the assemblages show low percentages of *Bitectatodinium tepikiense* but are otherwise characterized by similar fluctuations in the abundances of *Brigantedinium* spp., *Spiniferites* spp., and *Operculodinium centrocarpum* compared with the older Pleistocene intervals below. In their study of Hole 911A, Matthiessen and Brenner (1996) found that since ~1 Ma, the dinoflagellate cyst assemblages of the Yermak Plateau reveal a similarity in composition to Holocene assemblages from oceanic surface-water environments in the Norwegian-Greenland Sea and eastern Arctic Ocean. In overall character, the contemporaneous in situ assemblages at Site 986 are comparable to those of the Yermak Plateau. The assemblages differ, however, in containing high proportions of reworked Cenozoic and Mesozoic dinoflagellate cysts. A marked abundance peak of *O. centrocarpum* is observed between 66.04 and 58.04 mbsf at Site 986. A similar distinct acme of *O. centrocarpum* is recorded at 98.95 mbsf in Hole 911A. The dominance of *O. centrocarpum* at this stratigraphic level on the Yermak Plateau suggests an episode with increased influence of the North Atlantic Current and West Spitsbergen Current at around 0.5 Ma.

The low-resolution sampling at Site 986 does not allow identification of any small-scale cycles through the upper Pliocene–Pleistocene. The low abundance and diversity at 30.24 mbsf is attributed to glacial conditions, whereas the increase in the relative abundance of *O. centrocarpum* and *Spiniferites* spp. between 11.24 and 3.74 mbsf may imply a new retreat of ice-dominated waters in the northern Atlantic-Arctic region. According to Lloyd et al. (1996), initial deglaciation of the Spitsbergen margin occurred at 14.1 ka. These authors, however, found no evidence of an influx of warmer subpolar waters during this time. Lloyd et al. (1996) further determined that the first influx of subpolar North Atlantic waters into the area was during the second deglacial phase of the Spitsbergen ice mass at the beginning of the Holocene. This episode, dated at ~9 ka, was as warm as if not warmer than the present day along the Spitsbergen margin. The sample at 3.74 mbsf can probably also be related to this warming event. More detailed analyses, however, are required to confirm this and to detect the high-frequency glacial–interglacial cycles through the Pleistocene succession at Site 986.

SUMMARY AND CONCLUSIONS

Dinoflagellate cyst analysis of the upper Pliocene–Pleistocene succession at Site 986 provides information that aids age interpretations of the seismic sequences. This information can also be used to interpret changes in depositional environments and paleoceanographic conditions along the western Svalbard margin during the last 2.6 Ma.

More than 290 taxa have been identified from Hole 986C, and 208 different taxa have been recovered from Hole 986D. Most of these taxa are reworked from older Neogene, Paleogene, and Mesozoic deposits. The low thermal maturity and good preservation of the reworked palynomorphs suggest a provenance area on the central or eastern Barents Shelf and/or eastern Svalbard. Most probably the reworked material followed a westerly drainage route into the Storfjorden Trough and was subsequently transported with the West Spitsbergen Current to the present deposition site.

The biostratigraphic occurrence of selected Pliocene–Pleistocene dinoflagellate species, together with data from magnetostratigraphy (Channell et al., Chap. 10, this volume) and foraminifers (Eidvin and Nagy, Chap. 1, this volume), provides information on the ages of the seismic sequences recognized at the drill site. The following events, among others, have been considered: (1) The LADs of *Selenopemphix brevispinosa* at 928.34 mbsf and *Invertocysta lacrymosa* at 909.14 mbsf, suggesting ages between 2.6 and 2.7 Ma for the oldest parts of the drilled succession; (2) an acme of *Filisphaera filifera* s.l. at 804.84 mbsf, possibly giving an age in the range of 1.9–2.1 Ma based on correlation with Hole 911A; (3) the LAD of *Sumatradinium pliocenicum* at 564.44 mbsf, indicating an age not younger than 1.65 Ma; (4) the LAD of *Amiculosphaera umbracula* at 333.53 mbsf, indicating an age of 1.5? Ma; and (5) the LAD of *Operculodinium israelianum* at 122.18 mbsf, suggesting an age of 0.73 Ma.

The distribution of dinoflagellate cysts at Site 986 is influenced by depositional processes attributed to the formation of a fan complex near the mouth of the Storfjorden Trough and climatological and oceanographic processes controlling the glacial buildup in the Barents Sea. Fluctuations in the relative abundance of various taxa and variations in the G:P ratio can be used to identify changes in the paleoenvironments through the upper Pliocene–Pleistocene succession. The dinoflagellate assemblages suggest a relatively strong influence

of the North Atlantic Current during periods of the late Pliocene–early Pleistocene and that relatively warm water was transported along the West Spitsbergen Current toward the Fram Strait. These periods of warm-water inflow must have alternated with periods of continuous sea-ice cover in the Arctic Ocean. The younger Pleistocene sediments are also characterized by marked fluctuations in the abundance of in situ dinoflagellate cysts. Intervals with low abundances are attributed to glacial stages. On the other hand, levels with increased abundances and diversities, combined with the occurrence of typical outer neritic to oceanic species, suggest periods with inflow of warmer North Atlantic surface-water masses. These warm events are noted at ~1.4–1.5, 1.2, and 0.5 Ma. Although the fluctuations in the distribution of dinoflagellates in the upper Pliocene–Pleistocene succession is clearly related to glacial–interglacial cycles, the low-resolution sampling at Site 986 does not allow further identification of high-frequency cycles through the late Neogene.

ACKNOWLEDGMENTS

Thanks are due to Astri Dugan, University of Oslo, for making the palynological preparations and to Berit Fossum, IKU Petroleum Research, for technical assistance with the illustrations. Figures 1 and 2 are kindly provided by NPD. The work has been carried out as a part of the IKU project 25.2451.00, supported by Norsk Hydro, Saga Petroleum, and Statoil. I also thank Rex Harland and Peta J. Mudie for helpful and valuable comments and suggestions as referees.

REFERENCES

Cronin, T.M., and Whatley, R., 1996. Ostracoda from Sites 910 and 911. *In* Thiede, J., Myhre, A.M., Firth, J.V., Johnson, G.L., and Ruddiman, W.F. (Eds.), *Proc. ODP, Sci. Results*, 151: College Station, TX (Ocean Drilling Program), 197–201.

Dale, B., 1996. Dinoflagellate cyst ecology: modelling and geological applications. *In* Jansonius, J., and McGregor, D.C. (Eds.), *Palynology: Principles and Applications.* Am. Assoc. Stratigr. Palynol. Found., 3:1249–1275.

de Vernal, A., Londeix, L., Mudie, P.J., Harland, R., Morzadec-Kerfourn, M.T., Turon, J.-L., and Wrenn, J.H., 1992. Quaternary organic-walled dinoflagellate cysts of the North Atlantic Ocean and adjacent seas: ecostratigraphy and biostratigraphy. *In* Head, M.J., and Wrenn, J.H. (Eds.), *Neogene and Quaternary Dinoflagellate Cysts and Arcritarchs:* Salt Lake City (Publisher's Press), 289–328.

Edwards, L.E., Mudie, P.J., and de Vernal, A., 1991. Pliocene paleoclimatic reconstruction using dinoflagellate cysts: comparison of methods. *Quat. Sci. Rev.*, 10:259–274.

Eidvin, T., Goll, R.M., Grogan, P., Smelror, M., and Ulleberg, K., 1998. The Pleistocene to middle Eocene stratigraphy and geological evolution of the western Barents Sea continental margin at well site 7316/5-1 (Bjørnøya West area). *Norsk Geologisk Tidsskrift*, 78:99–123.

Eidvin, T., Jansen, E., and Riis, F., 1993. Chronology of Tertiary fan deposits off the western Barents Sea: implications for the uplift and erosion history of the Barents shelf. *Mar. Geol.*, 112:109–131.

Eidvin, T., and Riis, F., 1989. Nye dateringer av de tre vestligste borehullene i Barentshavet. Resultater og konsekvenser for den tertiære hevningen. *Nor. Petrol. Direct.*, 27, 1–44.

Faleide, J.I., Solheim, A., Fiedler, A., Hjelstuen, B.O., Andersen, E.S., and Vanneste, K., 1996. Late Cenozoic evolution of the western Barents Sea-Svalbard continental margin. *Global Planet. Change*, 12:53–74.

Fiedler, A., 1992. Kenozoisk sedimentasjon i Lofotbassenget langs vestlige Barentshavmargin [Cand. Scient. Thesis]. Univ. of Oslo.

Funder, S., Abrahamsen, N., Bennike, O., and Feyling-Hanssen, R.W., 1985. Forested Arctic: evidence from North Greenland. *Geology*, 13:542–546.

Harland, R., 1984. Recent and late Quaternary dinoflagellate cysts from the area of the Greenland-Iceland-Faeroe-Scotland Ridge. *J. Micropalaeontol.*, 3:95–108.

Harland, R., 1988. Quaternary dinoflagellate cyst biostratigraphy of the North Sea. *Palaeontology*, 31: 877–903.

Harland, R., 1992. Dinoflagellate cyst biostratigraphy of the last 2.3 Ma from the Rockall Plateau, northeast Atlantic Ocean. *J. Geol. Soc. London*, 149:7–12.

Head, M.J., 1993. Dinoflagellates, sporomorphs, and other palynomorphs from the Upper Pliocene St. Erth Bed of Cornwall, southwestern England. *J. Paleontol. (Suppl.)* 67:1–62 (also *Paleontol. Soc. Mem.*, 31).

Head, M.J., 1996. Late Cenozoic dinoflagellates from the Royal Society borehole at Ludham, Norfolk, eastern England. *J. Paleontol.*, 70:543–570.

Hjelstuen, B.O., Elverhøi, A., Faleide, J.I., 1996. Cenozoic erosion and sediment yield in the drainage area of the Storfjorden Fan. *In* Solheim, A., Riis, F., Elverhoi, A., Faleide, J.I., Jensen, L.N., and Cloetingh, S. (Eds.), *Impact of Glaciations on Basin Evolution: Data and Models from the Norwegian Margin and Adjacent Areas.* Global Planet. Change, 12:95–117.

Jansen, E., Raymo, M.E., and Blum, P., et al., 1996. *Proc. ODP, Init. Repts.*, 162: College Station, TX (Ocean Drilling Program).

Larsen, H.C., Saunders, A.D., Clift, P.D., Beget, J., Wei, W., Spezzaferri, S., and the ODP Leg 152 Scientific Party, 1994. Seven million years of glaciation in Greenland. *Science*, 264:952–955.

Lentin, J.K., and Williams, G.L., 1993. *Fossil dinoflagellates: index to genera and species.* Contrib. Ser. Am. Assoc. Stratigr. Palynol., 28.

Lloyd, J., Kroon, D., Laban, C., and Boulton, G., 1996. Deglaciation history of the western Spitsbergen margin since the last glacial maximum. *In* Andrews, J.T., Austin, W.E.N., Bergsten, H., and Jennings, A.E. (Eds.), *Late Quaternary Palaeoceanography of the North Atlantic margins*, Geol. Soc. Am. Spec. Publ., 111:289–301.

Matthiessen, J., 1995. Distribution patterns of dinoflagellate cysts and other organic–walled microfossils in recent Norwegian–Greenland Sea sediments. *Mar. Micropaleontol.*, 24:307–334.

Matthiessen, J., and Brenner, W., 1996. Dinoflagellate cyst ecostratigraphy of Pliocene–Pleistocene sediments from the Yermak Plateau (Arctic Ocean, Hole 911A). *In* Thiede, J., Myhre, A.M., Firth, J.V., Johnson, G.L., and Ruddiman, W.F. (Eds.), *Proc. ODP, Sci. Results*, 151: College Station, TX (Ocean Drilling Program), 243–253.

McCarthy, F.M.G., and Mudie, P.J., 1996. Palynology and dinoflagellate biostratigraphy of upper Cenozoic sediments from Sites 898 and 900, Iberia Abyssal Plain. *In* Whitmarsh, R.B., Sawyer, D.S., Klaus, A., and Masson, D.G. (Eds.), *Proc. ODP, Sci. Results*, 149: College Station, TX (Ocean Drilling Program), 241–265.

Mørk, M.B.E., and Duncan, R.A., 1993. Late Pliocene basaltic volcanism on the Western Barents Shelf margin: implications from petrology and ^{40}Ar-^{39}Ar dating of volcaniclastic debris from a shallow drill core. *Nor. Geol. Tidsskr.*, 73:209–225.

Mudie, P.J., 1989. Palynology and dinocyst startigraphy of the Late Miocene to Pleistocene, Norwegian Sea ODP Leg 104, Sites 642 to 644. *Proceedings of the Ocean Drilling Program, Scientific Results*, 104: 587–610.

Mudie, P.J., 1992. Circum-Arctic Quaternary and Neogene marine palynofloras: paleoecology and statistical analysis. *In* Head, M.J., and Wrenn, J.H. (Eds.), *Neogene and Quaternary Dinoflagellate Cysts and Acritarchs.* Am. Assoc. Stratigr. Palynol. Foundation, 347–390.

Mudie, P.J., and Harland, R., 1996. Aquatic Quaternary. *In* Jansonius, J., and McGregor, D.C. (Eds.), *Palynology: Principles and Applications.* Am. Assoc. Stratigr. Palynol. Foundation, 2:843–877.

Myhre, A.M., and Eldholm, O., 1988. The western Svalbard margin (74°-80°N). *Mar. Pet. Geol.*, 5:134–156.

Nøttvedt, A., Berglund, L.T., Rasmussen, E., and Steel, R.J., 1988. Some aspects of the Tertiary tectonics and sedimentation along the western Barents Shelf. *In* Morton, A.C., and Parson, L.M. (Eds.), *Early Tertiary Volcanism and the Opening of the NE Atlantic*. Geol. Soc. Am. Spec. Publ., 39:421–425.

Osterman, L.E., 1996. Pliocene and Quaternary benthic foraminifers from Site 910, Yermak Plateau. *In* Thiede, J., Myhre, A.M., Firth, J.V., Johnson, G.L., and Ruddiman, W.F. (Eds.), *Proc. ODP, Sci. Results*, 151: College Station, TX (Ocean Drilling Program), 187–195.

Poulsen, N.E., Manum, S.B., Williams, G.L., and Ellegaard, M., 1996. Tertiary dinoflagellate biostratigraphy of Sites 907, 908, and 909 in Norwegian-Greenland Sea. *In* Thiede, J., Myhre, A.M., Firth, J.V., Johnson, G.L., and Ruddiman, W.F. (Eds.), *Proc. ODP, Sci. Results*, 151: College Station, TX (Ocean Drilling Program), 255–287.

Solheim, A., Riis, F., Elverhøi, A., Faleide, J.I., Jensen, L.N., and Cloetingh, S., 1996 (Eds.). Impact of glaciations on basin evolution: data and models from the Norwegian Margin and adjacent areas. *Global Planet. Change*, 12:1–450.

Spiegler, D., 1996. Planktonic foraminifer Cenozoic biostratigraphy of the Arctic Ocean, Fram Strait (Sites 908–909), Yermak Plateau (Sites 910–912), and East Greenland Margin (Site 913). *In* Thiede, J., Myhre, A.M.,

Firth, J.V., Johnson, G.L., and Ruddiman, W.F. (Eds.), *Proc. ODP, Sci. Results*, 151: College Station, TX (Ocean Drilling Program), 153–167.

Sundvor, E., and Eldholm, O., 1979. The western and northern margin off Svalbard. *Tectonophysics*, 59:239–250.

Sættem, J., Bugge, T., Fanavoll, S., Goll, R.M., Mørk, A., Mørk, M.B.E., Smelror, M., and Verdenius, J.G., 1994. Cenozoic margin development and erosion of the Barents Sea: core evidence from southwest of Bjørnøya. *Mar. Geol.*, 118:257–281.

Thiede, J., and Myhre, A.M., 1996. The paleoceanographic history of the North Atlantic–Arctic Gateways: synthesis of the Leg 151 drilling results. *In* Thiede, J., Myhre, A.M., Firth, J.V., Johnson, G.L., and Ruddiman, W.F. (Eds.), *Proc. ODP, Sci. Results*, 151: College Station, TX (Ocean Drilling Program), 645–658.

Van der Plas, L., and Tobi, A.C., 1965. A chart for judging the reliability of point counting results. *Am. J. Sci.*, 263:87–90.

Versteegh, G.J.M., 1997. The onset of major Northern Hemisphere glaciations and their impact on dinoflagellate cysts and acritarchs from the Singa section, Calabria (southern Italy) and DSDP Holes 607/607A (North Atlantic). *Mar. Micropaleontol.*, 30:319–343.

Wall, D., Dale, B., Lohmann, G.P., and Smith, W.K., 1977. The environmental and climatic distribution of dinoflagellate cysts in modern marine sediments from regions in the North and South Atlantic Oceans and adjacent seas. *Mar. Micropaleontol.*, 2:121–200.

Willard, D.A., 1996. Pliocene–Pleistocene pollen assemblages from the Yermak Plateau, Arctic Ocean: Sites 910 and 911. *In* Thiede, J., Myhre, A.M., Firth, J.V., Johnson, G.L., and Ruddiman, W.F. (Eds.), *Proc. ODP, Sci. Results*, 151: College Station, TX (Ocean Drilling Program), 297–307.

Wrenn, J.H., and Kokinos, J.P., 1986. Preliminary comments on Miocene through Pleistocene dinoflagellate cysts from De Soto Canyon, Gulf of Mexico. *In* Wrenn, J.H., Duffield, S.L., and Stein, J.A. (Eds.), *Am. Assoc. Stratigr. Palynol. Contrib. Ser.*, 17:169–225.

Zonneveld, K.A.F., and Bossenkool, K.P.,1996. Palynology as a tool for land-sea correlation: an example from the eastern Mediterranean region. *In* Andrews, J.T., Austin, W.E.N., Bergsten, H., and Jennings, A.E. (Eds.), *Late Quaternary Palaeocenography of the North Atlantic Margins.* Geol. Soc. Am. Spec. Publ., 111:351–357.

Date of initial receipt: 9 September 1997
Date of acceptance: 3 March 1998
Ms 162SR-011

Table 1. Palynological samples from Holes 986C and 986D.

Core, section, interval (cm)	Depth (mbsf)
162-986C-	
1H-3, 74-79	3.74
2H-3, 74-76	11.24
3H-3, 74-79	20.74
4H-3, 74-79	30.24
5H-3, 74-79	38.42
6H-2, 74-79	47.74
7H-3, 74-79	58.04
8H-3, 74-79	66.04
10X-3, 74-78	84.34
11X-3, 74-79	93.94
12X-3, 74-79	103.02
13X-3, 74-79	113.24
14X-3, 74-79	122.18
15X-3, 74-79	132.03
16X-3, 74-79	141.89
17X-3, 74-79	151.84
19X-2, 74-79	169.64
20X-2, 74-76	179.34
21X-3, 74-79	190.44
22X-3, 74-79	200.04
24X-1, 74-79	216.24
26X-1, 74-79	235.44
27X-1, 74-79	245.04
28X-1, 76-81	254.76
29X-3, 74-79	262.74
30X-3, 74-79	267.34
31X-3, 74-79	276.94
34X-1, 74-78	302.84
35X-1, 74-76	312.44
36X-1, 26-30	321.56
37X-3, 74-76	333.53
38X-3, 74-76	344.34
39X-3, 74-76	353.94
40X-3, 74-76	363.54
41X-3, 74-74	373.14
42X-3, 74-76	382.84
43X-3, 74-76	392.84
44X-3, 74-76	402.04
162-986D-	
2R-3, 74-79	401.14
6R-1, 74-76	436.64
8R-1, 74-79	455.84
9R-1, 22-24	464.92
11R-1, 28-32	484.18
14R-3, 74-79	516.44
15R-3, 74-79	526.04
16R-3, 74-79	535.64
17R-3, 74-79	545.24
18R-3, 74-79	554.84
19R-3, 74-79	564.44
21R-3, 74-79	583.74
27R-1, 29-31	637.99
28R-3, 74-79	651.14
29R-3, 74-79	660.64
30R-3, 78-83	670.38
31R-3, 74-79	679.94
32R-3, -74-79	689.54
33R-1, 74-78	696.14
34R-2, 74-79	707.24
35R-3, 74-79	718.34
37R-3, 74-79	737.54
38R-3, 74-79	747.14
39R-3, 74-79	756.74
40R-3, 74-79	766.34
41R-3, 74-79	775.94
42R-3, 74-79	785.54
43R-3, 64-68	795.04
44R-3, 74-79	804.84
45R-3, 74-79	814.44
46R-3, 74-79	824.04
47R-1, 74-79	830.64
48R-2, 74-79	841.74
49R-1, 74-79	849.94
50R-2, 74-79	861.04
51R-4, 74-79	873.46
52R-4, 74-79	883.34
53R-3, 74-79	891.34
54R-1, 74-79	898.04
55R-2, 74-79	909.14
59R-1, 74-79	946.04
60R-1, 74-79	955.74

Plate 1. Scale bar = 25 µm. All photos are interference contrast except figure 12, which is phase contrast. EFC = England Finder coordinates. **1.** *Bitectatodinium tepikiense,* Sample 162-986D-19R-3, 74–79, 564.44 mbsf, EFC M37/0. **2.** *Brigantedinium* sp., Sample 162-986C-8H-3, 74–79, 66.04 mbsf, O47/0. **3.** *Nematosphaeropsis labyrinthus,* Sample 162-986C-22X-3, 74–79, 200.04 mbsf, EFC P32/2. **4.** *Operculodinium israelianum,* Sample 162-986D-21R-3, 74–79, 583.74 mbsf, EFC N39/0. **5.** *Multispinula quanta,* Sample 162-986C-8H-3, 74–79, 66.04 mbsf, EFC K42/3. **6.** *Nematosphaeropsis labyrinthus,* Sample 162-986C-22X-3, 74–79, 200.04 mbsf, EFC P32/2. **7.** *Operculodinium israelianum,* Sample 162-986D-21R-4, 74–79, 583.74 mbsf, EFC N39/0. **8.** *Impagidinium pallidum,* Sample 162-986D-57R-2, 74–79, 928.34 mbsf, EFC P35/2. **9.** *Algidasphaeridium*? *minutum,* Sample 162-986D-11R-1, 28–32, 484.18 mbsf, EFC S41/4. **10.** *Algidasphaeridium*? *minutum,* Sample 162-986D-11R-1, 28–32, 484.18 mbsf, EFC 031/3. **11.** *Filisphaera filifera* s.l., Sample 162-986D-15R-3, 74–79, 526.04 mbsf, EFC K34/1. **12.** *Filisphaera filifera* s.l., Sample 162-986D-15R-3, 74–79, 526.04 mbsf, EFC M32/3. **13.** *Amiculosphaera umbracula,* Sample 162-986D-15R3, 74–79, 526.04 mbsf, EFC T33/4. **14.** *Achomosphaera andalousiensis,* Sample 162-986C-22X-3, 74–79, 200.04 mbsf, EFC C35/2. **15.** *Selenopemphix nephroides,* Sample 162-986C-8H-3, 74–79, 66.04 mbsf, EFC Q36/4. **16.** *Sumatradinium pliocenicum,* Sample 162-986D-21R-3, 74–79, 583.74 mbsf, EFC L33/0.

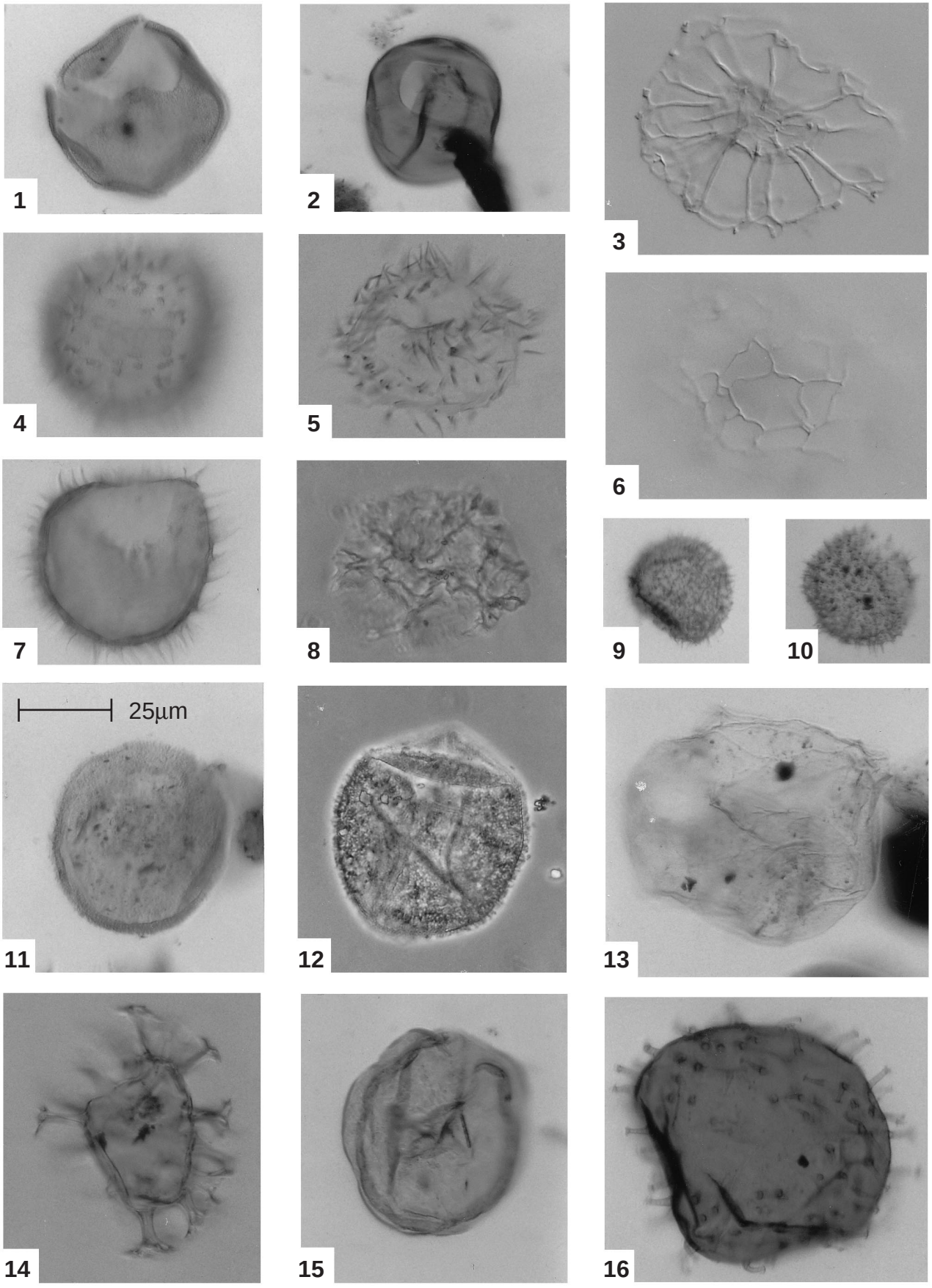
1
2
3
4
5
6
7
8
9
10
25µm
11
12
13
14
15
16